

PEGylation affects the self-assembling behavior of amphiphilic octapeptides

Diego Romano Perinelli¹, Mario Campana², Ishwar Singh³, Driton Vllasaliu⁴, James Douch², Giovanni Filippo Palmieri¹, Luca Casettari^{*5}

¹School of Pharmacy, University of Camerino, via Gentile III da Varano, 62032 Camerino, MC, Italy.

²ISIS Neutron Facility, Science and Technology Facilities Council, Rutherford Appleton Laboratory, Didcot OX11 0QX, United Kingdom

³School of Pharmacy, University of Lincoln, Green Lane, Lincoln, LN6 7DL, UK

⁴King's College London, Institute of Pharmaceutical Science, London SE1 9NH, UK

⁵Department of Biomolecular Sciences, University of Urbino Carlo Bo, Piazza del Rinascimento, 6, 61029 Urbino (PU), Italy.

ABSTRACT

Surfactant-like peptides are a class of amphiphilic macromolecules, which are able to self-assemble in water forming different supramolecular structures. Among them, octapeptides composed of six hydrophobic and two hydrophilic residues have attracted interest since they have a length similar to those of natural phospholipids. Supramolecular structures of different amphiphilic octapeptides have been widely reported, but no study has been performed aimed at investigating the effect of PEGylation on their self-assembling behaviour. The aim of the present work was to synthesize and characterise the self-assembling behaviour of PEGylated alanine- or valine based amphiphilic octapeptides (mPEG_{1.9kDa}-DDAAAAAA and mPEG_{1.9kDa}-DDVVVVVV) in comparison to the non-PEGylated ones (DDAAAAAA and DDVVVVVV).

The self-aggregation process in ultrapure water was investigated by fluorescence spectroscopy, small angle neutron scattering (SANS), dynamic light scattering (DLS), while the secondary structure was assessed by circular dichroism.

PEGylation markedly affects the self-assembling behaviour of these amphiphilic octapeptides in terms of both critical aggregation concentration (CAC) and shape of the formed supramolecular aggregates. Indeed, PEGylation increases CAC and prevents the self-aggregation into fibrillary supramolecular aggregates (as observed for non-PEGylated peptides), by promoting the formation of micelle-like structures (as demonstrated for valine-based octapeptide).

34 On the other side, the secondary structure of peptides seems not to be affected by PEGylation. Overall,
35 these results suggest that self-assembling behaviour of amphiphilic octapeptides can be modified by
36 PEGylation, with a great potential impact for the future applications of these nanomaterials.

37

38 **KEYWORDS:** surfactant-like peptides, PEGylated peptides, nanostructures, small angle neutron
39 scattering (SANS), micelles.

40

41

42

43

44

45

46

47

48

49

50

51

52

53

54

55

56

57

58

59

60

61

62

63

64

65

66

67

68 INTRODUCTION

69 In recent years, molecular self-assembly of peptides has attracted great interest due to wide potential
70 applications in nanotechnology and nanomedicine for the design of nanostructured smart materials ¹.

71 The amphiphilic self-assembled peptides are termed as “*surfactant-like peptides*”. They are composed
72 of a sequence of consecutive hydrophobic amino acids as the tail and one or two hydrophilic amino
73 acids as the head ². Generally, the hydrophobic sequences contain glycine (G), alanine (A), valine
74 (V), leucine (L) or isoleucine (I) residues, while the hydrophilic heads are made up of negatively (i.e.
75 aspartic (D) or glutamic acid (E)) or positively (i.e. lysine (K), histidine (H) or arginine (R)) charged
76 amino acids. The hydrophobic tail of a surfactant-like peptide is composed of six to nine hydrophobic
77 residues, so that it is similar to the length of natural phospholipids (around 2.5-3 nm).

78 Valine and alanine residues are preferred to glycine, leucine and isoleucine residues since they
79 produce more homogeneous and stable structures, probably due to the formation of stronger β -sheet
80 elements ³.

81 The self-assembling properties of these materials can be tuned by changing the peptide sequences,
82 both in the hydrophobic and hydrophilic region, giving a range of supramolecular architectures,
83 including nanotubes, nanovesicles or nanofibers. Upon dissolution in water (4-5 mM), negatively
84 charged peptides, such as Ac-A6D, Ac-V6D, Ac-G8DD or KV6, are able to form open-ended
85 nanotubes with 30-50 nm of diameter and different lengths up to 1 μm ⁴.

86 The amphiphilic sequences consisting of alanine, valine and glutamic acid can be coupled with other
87 materials to produce nanostructures with a wide range of applications. In one such example, these
88 sequences were coupled with a palmitoyl chain to form fibrillar nanostructures as promising
89 biomimetic hydrogel scaffolds ⁵. In fact, Pashuck et al. observed that the arrangement of the
90 hydrophobic residues not only affects the supramolecular structures but also the stiffness of the
91 obtained hydrogel as a function of the total number of the hydrophobic residues and the strength of
92 the β -sheet regions. The functionalization with lipids was also found to increase the *in vivo* stability
93 of peptides.

94 Apart from the modification with lipids, no other chemical functionalization of these alanine, valine
95 or glutamic based amphiphilic peptides is reported in the literature.

96 PEGylation is a common and well known strategy to improve water solubility and stability of
97 peptides, and PEGylated peptides offer other advantages following *in vivo* administration, including
98 increased plasma half-life and reduced immunogenicity ⁶.

99 Different studies were recently performed on a tetra-phenylalanine peptide linked to PEGs with
100 different molecular weights (5 kDa, 1.8 kDa, 1.2 kDa and 350 Da) to investigate the self-assembling
101 behaviour in aqueous solution ⁷⁻¹⁰. As an example, amphiphilic 3-helix PEGylated lipopeptides were

102 synthesized and were found to self-assemble into monodisperse micellar nanoparticles of 15 nm
103 diameter. After loading with doxorubicin, used as model anticancer drug, they showed minimal
104 leakage after 12 h of incubation with serum proteins at 37 °C. Moreover, the in vivo half-life was
105 29.5 hours and minimal accumulation in the liver and spleen was observed using positron emission
106 tomography ¹¹.

107 Despite the well-established beneficial attributes and improved performances imparted by
108 PEGylation on different peptides, no study has been focused on the effect of PEGylation on the self-
109 assembling behaviour of surfactant-like octapeptides. Thus, the aim of this work was to synthesize
110 and investigate for the first time the self-assembling behaviour in water of PEGylated alanine- and
111 valine-based surfactant-like octapeptides (mPEG_{1.9kDa}-DDAAAAAA and mPEG_{1.9kDa}-
112 DDVVVVVV) and to compare them with the non-PEGylated ones (DDAAAAAA and
113 DDVVVVVV).

114

115 **EXPERIMENTAL SECTION**

116

117 Synthesis of amphiphilic octapeptides

118

119 All peptides were synthesized through the solid phase automated microwaved-assisted approach
120 starting from protected amino acid Fmoc-ALA-OH (Fluorochem, UK), Fmoc-VAL-OH
121 (Fluorochem, UK) Fmoc-ASP(otbu)-OH (Fluorochem, UK). Rink amide ChemMatrix (Biotage, NC,
122 USA) was used as resin. For the amino acid sequence, the coupling agents were Ethyl 2-cyano-2
123 (hydroxyimino) acetate (Oxyma; Fluorochem, UK) and N, N'-Diisopropylcarbodiimide (DIC;
124 Fluorochem, UK). Coupling were performed at 75 °C for 5 minutes from the first to the fourth amino
125 acid, for 7 minutes from the fifth and sixth amino acid and for 10 minutes for the last two amino
126 acids. Subsequently, carboxylic-ended poly(ethylene glycol) monomethyl ether (1.9 kDa) was
127 coupled to the amino end of the amino acid sequence attached to the resin. Carboxylic-ended
128 poly(ethylene glycol) monomethyl ether was synthesized from mPEG (1.9 kDa; Polysciences Europe,
129 Germany). For the synthesis, mPEG was functionalised on the free hydroxyl group with glutaric
130 anhydride (Sigma Aldrich, Italy), using 4-Dimethylaminopyridine (DMAP, Sigma Aldrich, Italy) as
131 organocatalyst, in dichloromethane, to obtain a carboxylic end. After the reaction, the polymer was
132 purified by dialysis using 1 kDa MWCO membrane (Spectra/Por[®], USA).

133 Carboxylic-ended poly(ethylene glycol) monomethyl ether was characterised by ¹H-NMR and gel
134 permeation chromatography (GPC) analysis (M_n 1842; M_w 2005; PDI 1,088). The Carboxylic-ended
135 poly(ethylene glycol) monomethyl ether coupling was performed using 1-

136 [Bis(dimethylamino)methylene]-1H-1,2,3-triazolo[4,5-b]pyridinium 3-oxid hexafluorophosphate
137 (HATU, Sigma-Aldrich, UK) and N,N-Diisopropylethylamine (DIPEA; Sigma-Aldrich, UK) at 75
138 °C for 10 minutes. After cleavage from the resin with trifluoroacetic acid (Fluorochem, UK), peptides
139 were precipitated in cold diethyl ether. The raw materials were purified through RP-HPLC (Thermo
140 Scientific Dionex Ultimate 3000 RP-HPLC equipped with a Phenomenex Gemini NX C18 110 Å,
141 150 x 4.6 mm) column, using the following buffer systems: A: 50 mM ammonium carbonate, B:
142 acetonitrile and a flow rate of 1 ml/min. The following gradient was applied: 95% A for 2 min; 5-
143 95% B in 25 min; 95% B for 5 min.

144

145 Mass analysis

146 For electron spray mass ionization (ESI) analysis, approximately 1 mg of each peptide was dissolved
147 in ultrapure water and analysed by direct injection in an ESI mass apparatus (HP 1100 LC/MSD,
148 Agilent) equipped with a single quadrupole detector. The sample was analysed in the positive mode
149 at a fragmentor voltage of 30 V.

150 MALDI-TOF spectra were acquired on a 400 Plus MALDI TOF/TOF Analyzer (AB Sciex, MA,
151 USA). Peptides were dissolved in ultrapure water with 0.05% TFA and mixed, in the same volumetric
152 amount, with the saturated matrix solution (2, 5-Dihydroxybenzoic acid saturated solution in 50:50,
153 0.05% TFA water/acetonitrile). 1 µL of this solution was applied onto the MALDI sample plate and
154 allowed to co-crystallize at room temperature and then analysed at a 6000 laser intensity.

155

156 Circular Dichroism (CD)

157 Far UV CD spectra of peptides were collected using a π^* -180 step-flow spectrometer (Applied
158 Photophysics, Leatherhead, UK). Peptides were analysed dissolved in ultrapure water at a
159 concentration of 1 mg/mL for non-PEGylated and 3 mg/mL for PEGylated peptides. Spectra were
160 recorded in the range of 180-280 nm with a step of 0.1 nm and a bandwidth of 1 nm. The acquisition
161 time was 2 s for each point. A 10 mm path length quartz cuvette was filled with the peptide solution
162 and measured at room temperature.

163

164 Critical aggregation concentration (CAC)

165 Steady-state fluorescence spectra of pyrene in the presence of different concentration of non-
166 PEGylated or PEGylated peptides were recorded at 37 °C using a spectrofluorimeter (LS-55, Perkin-
167 Elmer) equipped with a thermostated cell (HAAKE C25P thermostat). The fluorescence emission

168 spectra (350–600 nm) of pyrene were measured using an excitation wavelength $\lambda_{\text{exc}} = 338$ nm and
169 2.5 nm slits. The intensity ratio of the first (I) and third (III) vibronic band of the emission spectrum
170 of pyrene, at 372 nm and 384 nm, was plotted against the peptide concentration. The critical
171 aggregation concentration (CAC) of peptides was determined by fitting the experimental data with
172 the following equation (GraphPad Prism 6):

$$173 \quad Y = \frac{\text{Bottom} + (\text{Top} - \text{Bottom})}{1 + 10^{[(\text{LogCMC} - x) * \text{Hill slope}]}}$$

174 where Top and Bottom are the plateau of the curve in the unit of Y axis, hill slope is the steepness of
175 the curve.

176

177 Small angle neutron scattering (SANS)

178 SANS data were collected on the LOQ small-angle diffractometer at the ISIS Pulsed Neutron Source
179 (STFC Rutherford Appleton Laboratory, Didcot, U.K.), using a two-dimensional, position-sensitive,
180 ^3He detector neutron detector to provide a simultaneous Q range of 0.08–2 nm⁻¹ ^{12,13}. Each sample
181 and solvent (D₂O for background) was placed in 2 mm path length quartz banjo cuvettes and measured
182 for a total of 2 hours in order to gather data of high statistical precision. Each raw scattering data set
183 was then corrected for the detector efficiencies, sample transmission and background scattering and
184 converted to scattering cross-section data ($\partial\Sigma/\partial\Omega$ vs Q) using the instrument-specific software
185 (MantidPlot) ¹⁴. Non-PEGylated peptides were analysed at 5 mg/mL, while PEGylated peptides at 30
186 mg/mL in ultrapure water at 37 °C. The temperature was controlled by using a thermostat (Julabo
187 bath) with a precision of 0.1 °C. SANS data were analysed using SASview 4.1 software.

188

189 Dynamic light scattering (DLS)

190 The hydrodynamic diameter (nm) and size distribution (width; nm) of non-PEGylated and PEGylated
191 peptides were determined by DLS from the size by intensity (%) traces. DLS measurements were
192 carried out using a Zetasizer Nano S (Malvern Instruments, UK) that employs a 173° backscatter
193 detector. For the analysis, samples were loaded inside disposable cuvette and equilibrated 300 s at
194 the operating temperature. The operating settings were position (mm): 4.65; attenuator: 11 and
195 temperature: 37 °C.

196

197

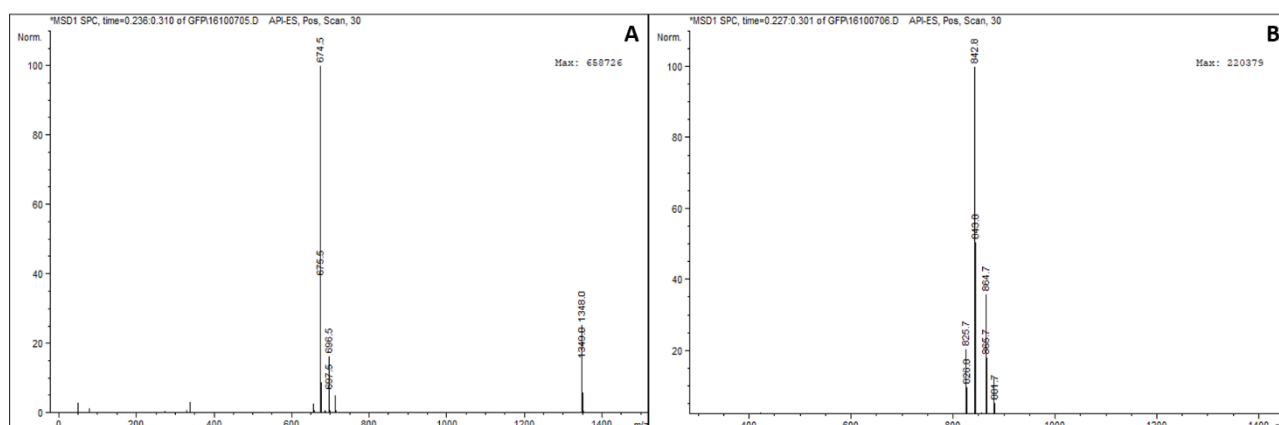
198 **RESULTS AND DISCUSSION**

199

200 All synthesized peptides were characterized by mass analysis. Mass analysis is a standard technique
201 employed for the identification and determination of the eventual presence of impurities in the
202 sample. ESI mass spectra (positive mode) indicate the purity of non-PEGylated peptides. In mass
203 spectra, only one molecular ion (m/z) and the relative adduct ions can be recognized. For
204 DDAAAAAA the molecular ion is at 674.5 m/z , while for DDVVVVVV the molecular ion is at 842.8
205 m/z (**Figure 1**). These mass values are comparable to those theoretically calculated for these peptide
206 sequences.

207

208

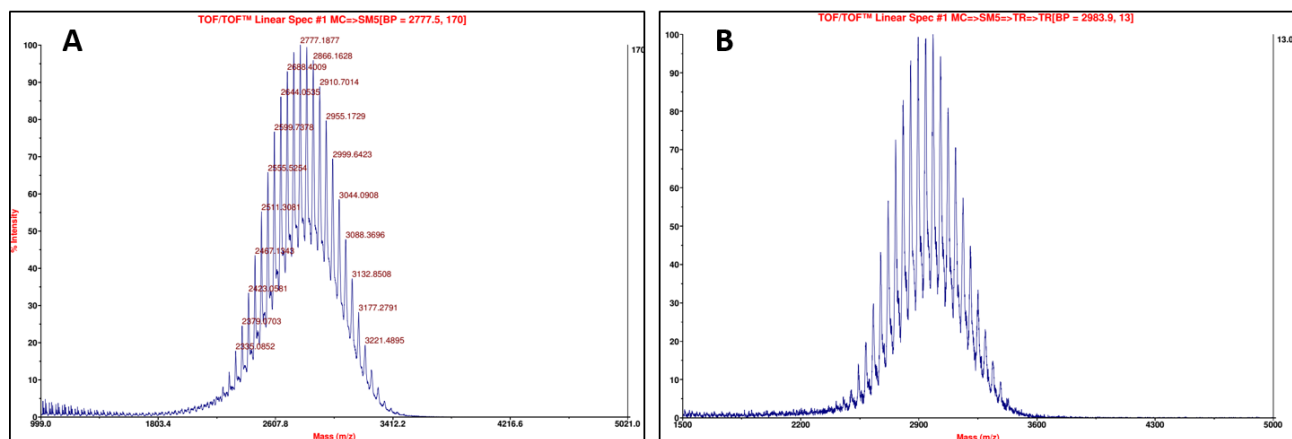


209 **Figure 1** ESI mass spectra of non-PEGylated amphiphilic octapeptides: DDAAAAAA (A) and
210 DDVVVVVV (B).

211

212 Due to the higher molecular weight (above 1000 Da), no reliable results were obtained from ESI mass
213 analysis of PEGylated peptides. Specifically, a large number of fragment ions below 1000 Da were
214 observed, which were not unambiguously assigned to the sample. Therefore, PEGylated peptides were
215 subsequently analysed by MALDI-TOF. A single molecular weight distribution can be observed in
216 the analysed mass range 1-5 kDa for both PEGylated peptides, referring to the PEGylated adducts, as
217 demonstrated from the calculated average molecular weights (2778 Da for mPEG_{1.9kDa}-DDAAAAAA
218 and 2984 Da for mPEG_{1.9kDa}-DDVVVVVV) (**Figure 2**).

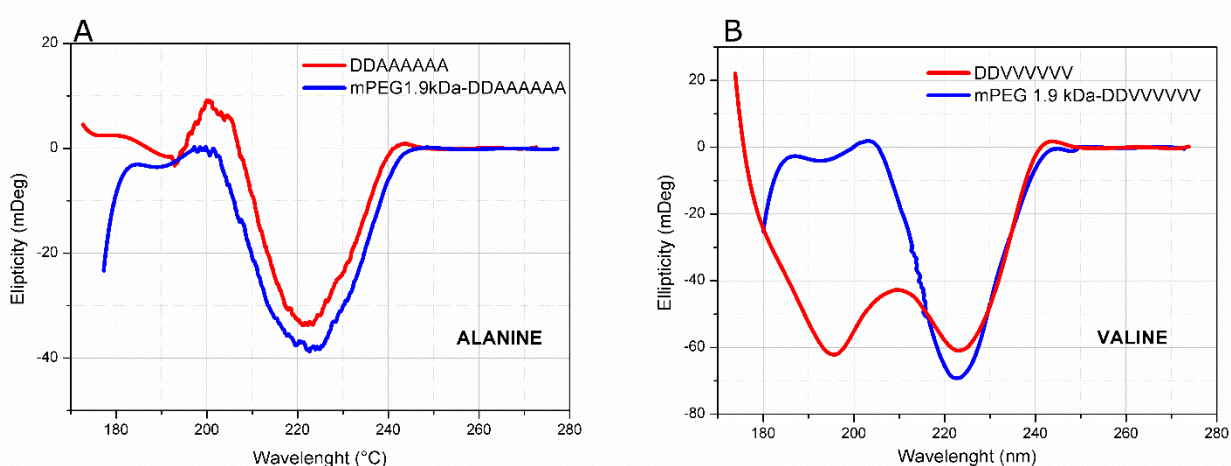
219



220
 221 **Figure 2** MALDI-TOF mass spectra of PEGylated amphiphilic octapeptides: mPEG_{1.9kDa}-
 222 DDAAAAAA (A) and mPEG_{1.9kDa}-DDVVVVVV (B).

223
 224

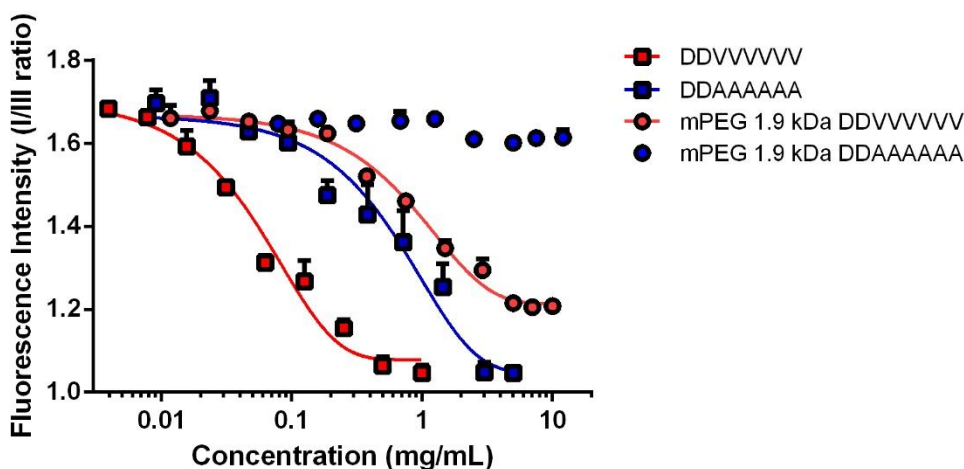
225 The secondary structure in aqueous dispersion of peptides was investigated by circular dichroism. As
 226 for other valine and alanine based-peptides¹⁵⁻¹⁷, this analysis confirmed that the amphiphilic peptides
 227 assume predominantly a beta-sheet conformation in water, as indicated by a minimum in ellipticity
 228 at around 220 nm. An appreciable fraction of random coil was only observed for the non-PEGylated
 229 valine peptide (DDVVVVVV) due to the presence of a minimum at around 190-200nm. Random coil
 230 fraction was negligible for the other peptides. Notably, PEGylation does not affect the secondary
 231 structure of peptides since PEGylated amphiphilic octapeptides (DDAAAAAA and DDVVVVVV)
 232 maintains the beta-sheet conformation as the non-PEGylated ones (**Figure 3**).



233
 234 **Figure 3** CD spectra of alanine-based (DDAAAAAA and mPEG_{1.9 kDa}-DDAAAAAA) peptides (A)
 235 and valine-based (DDVVVVVV and mPEG_{1.9 kDa}-DDVVVVVV) peptides (B).

236

237 The critical aggregation concentration (CAC) values of the synthesized peptides were calculated by
 238 steady state fluorescence from the I/III peak ratio of pyrene, used as a probe. This ratio is particularly
 239 sensitive to the polarity of the microenvironment around the probe, which decreases at a peptide
 240 concentration at which the aggregation process begins. The calculated CAC values were $0.055 \pm$
 241 0.003 mg/mL (0.065 mM; $R^2 = 0.993$) for DDVVVVVV; 0.906 ± 0.047 mg/mL (1.3 mM; $R^2 = 0.982$)
 242 for DDAAAAAAAA; 1.638 ± 0.402 mg/mL (0.6 mM; $R^2 = 0.994$) for mPEG_{1.9kDa}-DDVVVVVV. No
 243 changes in the I/III fluorescence ratio were observed for mPEG_{1.9kDa}-DDAAAAAAAA at the tested
 244 concentrations, suggesting no aggregation process. The results clearly indicated the effect of peptide
 245 sequence and PEG-coupling on CAC. Particularly, the lower CAC values for DDVVVVVV peptide
 246 in comparison to DDAAAAAAAA peptides are related to the higher hydrophobicity of valine residues.
 247 On the other hand, PEGylation has an opposite effect by inducing an increase in the self-aggregation
 248 concentration of the analysed peptides. The lower fluorescence intensity I/III ratio reached for
 249 concentrations of non-PEGylated peptides above CAC, in comparison to mPEG_{1.9kDa}-DDVVVVVV,
 250 indicates a more hydrophobic environment of the core compared to that of aggregates formed by the
 251 analysed PEGylated peptide (Figure 4).



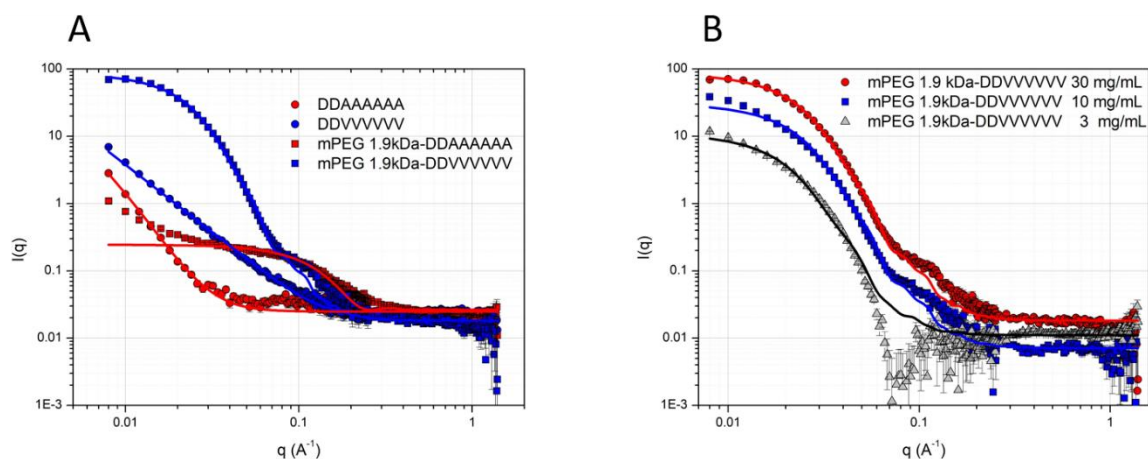
252

253 **Figure 4** Variation of fluorescence intensity for the ratio between vibrionic peak I (λ 372 nm) and
 254 peak III (λ 384 nm) of pyrene as a function of concentration for non-PEGylated (DDAAAAAAAA and
 255 DDVVVVVV) and PEGylated (mPEG_{1.9kDa}-DDAAAAAAAA and mPEG_{1.9kDa}-DDVVVVVV)
 256 octapeptides.

257

258 The fitting of SANS profiles related to the PEGylated peptides, using the ellipsoid model, revealed
 259 the formation in aqueous dispersion of micellar-type aggregates with an elongated shape. The
 260 calculated radii were 5.1 nm (polar) and 11.7 nm (equatorial) for mPEG_{1.9kDa}-DDVVVVVV and 1.8

261 nm (polar) and 1.7 nm (equatorial) for mPEG_{1.9kDa}-DDAAAAAA. This result highlighted a self-
 262 assembling process only for the PEGylated valine-based peptide and not for the alanine-based peptide
 263 at the tested concentration, confirming the results obtained from fluorescence spectroscopy using
 264 pyrene as a probe. On the contrary, non-PEGylated peptides showed a different scattering profiles
 265 which can be attributed to fibrillary structures of larger dimensions. DDVVVVVV profiles can be
 266 fitted with a lamellar model with a thickness of 2.8 nm, while for DDAAAAAA the lamellar thickness
 267 was around 12.0 nm. The higher computed polydispersity for DDAAAAAA with respect to
 268 DDVVVVVV peptides indicates the formation of less homogeneous structures for alanine based-
 269 peptides (**Figure 5A**). The mPEG_{1.9kDa}-DDVVVVVV peptide was also analysed at different
 270 concentrations above CAC (30 mg/mL, 10 mg/mL and 3 mg/mL). The fitting of the relative SANS
 271 profiles confirmed that the elongated shape of micellar aggregates for PEGylated valine octapeptide
 272 is maintained at all concentrations analysed above CAC (**Figure 5B**).



273

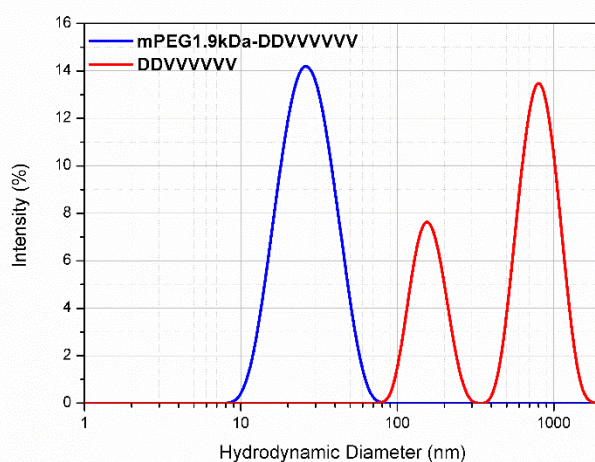
274 **Figure 5** SANS profiles for non-PEGylated (DDAAAAAA and DDVVVVVV) octapeptides at a
 275 concentration of 5 mg/mL and for PEGylated (mPEG_{1.9kDa}-DDAAAAAA and mPEG_{1.9kDa}-
 276 DDVVVVVV) octapeptides at a concentration of 30 mg/mL (A). SANS profiles for the mPEG_{1.9kDa}-
 277 DDVVVVVV octapeptide at different concentrations above CAC (30 mg/mL, 10 mg/mL and 3
 278 mg/mL) (B). Lines represent the fitted signals.

279

280

281 **Figure 6** shows the size distribution traces (intensity %) relative to the analysed PEGylated or non-
 282 PEGylated amphiphilic DDVVVVVV peptide. A smaller and monomodal particle size distribution
 283 was observed for the PEGylated peptide, with a calculated hydrodynamic diameter of 26.63 ± 0.41
 284 nm. This size value is comparable to that of spherical/elongated micelles and comparable with the

285 range of size (10-50 nm) reported for other PEGylated peptides^{18,19}. On the other hand, bimodal and
286 larger distributions were found for the non-PEGylated alanine based-peptide. The bimodal
287 appearance of DLS traces related to non-PEGylated amphiphilic peptides (DDVVVVVV) reflects the
288 possible non-spherical shape of these samples. DLS analysis in fact suggests the presence of at least
289 two dimensions, one significantly below 100 nm (approximately 35-40 nm) and another from 200 nm
290 to more than 1000 nm. This result can be explained by considering DDVVVVVV could form
291 fibrillary supramolecular structures, as reported in the literature for similar amphiphilic peptides^{20,21}.



292

293 **Figure 6** DLS traces of valine-based amphiphilic octapeptide at 25 °C before and after PEGylation
294 obtained at a concentration above CAC (5 mg/mL for DDVVVVVV and 30 mg/mL for mPEG_{1.9kDa}-
295 DDVVVVVV).

296

297 Surfactant-like peptides represent a class of amphiphilic macromolecules, which have been widely
298 characterized in terms of self-assembling behaviour. Amphiphilic peptides can form a number of
299 supramolecular structures in water (e.g. nanofibers, nanorods, nanovesicles) due to different possible
300 interactions between amino acid residues. Hydrogen bonds, van der Waals forces as well as
301 electrostatic, hydrophobic and/or aromatic interactions (π - π stacking) can all be involved in the self-
302 assembling process. The properties of these peptides can be tuned by changing the amino acid
303 sequence or by a further derivatization at the amino or carboxyl end groups, leading to the design of
304 novel functional biomaterials. In the field of drug delivery, peptides have been largely investigated
305 as potential macromolecules for the design of novel nanocarriers, since they display some advantages
306 over common synthetic surfactants. These include a better biocompatibility and the possibility of
307 inducing specific biological functions or controlling drug release and enhancing cell uptake in
308 response to stimuli, based on the amino acid sequence.

309 The drawbacks of nanosystems formed by the self-assembly of surfactant-like peptides however
310 include low stability in solution, poor aqueous solubility, potential heterogeneity of the
311 nanoassemblies and the low drug loading. To overcome some limitations of these nanocarriers,
312 hydrophilic peptides have been functionalized with fatty acids, to give rise to amphiphilic
313 macromolecules, known as peptide amphiphiles, which, at the moment, represent the most
314 investigated building blocks for the design of peptide-based nanocarriers.

315 Additional functionalization strategies of peptides are possible, which maintain the amphiphilic
316 character of these materials and the self-assembly ability. One of these is PEGylation. Covering the
317 surface of nanosystems with PEG is, indeed, a very common strategy to reduce immunogenicity,
318 thereby increasing the systemic circulation time. The use of PEGylated lipids to prepare PEGylated
319 liposomes (the so-called second generation or stealth liposomes) is an established practice.
320 PEGylation has also been demonstrated as an effective approach to improve the stability and
321 solubility of peptides in water. Despite these advantages, not enough attention has been focused on
322 the effect of PEGylation on the self-assembling behaviour.

323 Self-assembling is known to be affected by the secondary structure (e.g. α -helix, β -sheets) and the
324 obtained nanostructures (such as nanospheres, nanofibers, nanorods and nanotubes) are dependent on
325 the feature of the hydrophilic and hydrophobic portions of the material ²². Different works have
326 investigated the secondary structure of octapeptides ^{23,24}. Particularly for surfactant-like peptides
327 formed by six hydrophobic and one or two anionic residues, a β -sheet conformation has been reported
328 ²¹, which is probably related to the repetition of the hydrophobic residues such as alanine or valine,
329 owing to the stacking interaction via intermolecular hydrogen bonds ^{3,25}. In this work, a β -sheet
330 conformation was observed for DDAAAAAA and DDVVVVVV peptides, which was not affected
331 after conjugation with PEG. Actually, the effect of PEGylation on conformational stability of proteins
332 or peptides is not well clarified ²⁶. In some studies, no effect was observed on the secondary structure
333 of epta- or octapeptides after PEGylation ²⁷. No systematic studies can also be found in the literature
334 in which CAC of PEGylated peptides are compared with that of non-PEGylated counterparts.
335 Theoretically, PEGylation should increase the CAC value of peptides by increasing its hydrophilicity.
336 For instance, CAC values in the range of μ M up to 1-2 mM have been calculated for surfactant-like
337 peptides ²⁸⁻³⁰, and, generally, higher CAC values (in the range of mM) have been found for PEGylated
338 peptides ^{31,11}. SANS profiles confirmed the effect exerted by the coupling of 1.9kDa PEG to the
339 hydrophilic portion on the self-assembling behaviour of the investigated surfactant-like octapeptides.
340 We demonstrate that, PEGylation maintains the self-assembling properties only for the valine-based
341 octapeptide. This is different to the effect seen with alanine-based peptides, suggesting that the
342 coupling with 1.9kDa PEG confers a high level of hydrophilicity, which can be balanced only by the

343 higher hydrophobicity of valine compared to alanine residues. Moreover, PEGylation seems to induce
344 the formation of more homogeneous and elongated micelles, unlike non-PEGylated octapeptides for
345 which fibrillar or ribbon-like structures have been already reported³²⁻³⁴.

346

347 **CONCLUSIONS**

348 Overall, the results suggest that the PEGylation of amphiphilic alanine- or valine-based octapeptides
349 markedly affects their self-assembling behaviour in terms of critical aggregation concentration as
350 well as in terms of shape and structure of the formed supramolecular aggregates. Particularly,
351 PEGylation increases the CAC of these amphiphilic peptides and prevents the self-aggregation into
352 fibrillary aggregates. As evidenced by SANS and DLS, PEGylation promotes the formation of
353 elongated micellar structure for valine-based amphiphilic octapeptides, differently from the alanine-
354 based amphiphilic octapeptide, which does not self-assemble at the concentrations tested (up to 30
355 mg/mL). Conversely, PEGylation does not influence the secondary conformation of amphiphilic
356 octapeptides as evidenced by circular dichroism. Overall, these results suggest that PEGylation can
357 modify the self-assembling behaviour of amphiphilic octapeptides, leading to the formation of
358 different supramolecular aggregates. These findings can be helpful to enlarge the future applications
359 of these nanomaterials in different fields.

360

361

362 **AUTHOR INFORMATION**

363 Corresponding author

364 *E-mail: luca.casettari@uniurb.it

365

366 **ORCID**

367 Diego Romano Perinelli: 0000-0002-7686-4150

368 Mario Campana: 0000-0002-2151-4110

369 Ishwar Singh: 0000-0001-7822-1063

370 Driton Vllasaliu: 0000-0002-4379-6171

371 Giovanni Filippo Palmieri: 0000-0002-5349-4978

372 Luca Casettari: 0000-0001-6907-8904

373

374

375 ACKNOWLEDGMENT

376 SANS experiments at the ISIS Neutron and Muon Source were supported by a beamtime allocation
377 from the Science and Technology Facilities Council (UK).

378 The authors wish to thank Fabio De Belvis for the design and realization of the graphical abstract.

379

380

381 REFERENCES

- 382 (1) Akter, N.; Radiman, S.; Mohamed, F.; Reza, M. Self-Assembled Potential Bio Nanocarriers
383 for Drug Delivery. *Mini-Reviews Med. Chem.* **2013**, *13*, 1327–1339.
- 384 (2) Zhao, X. Design of Self-Assembling Surfactant-like Peptides and Their Applications. *Curr.*
385 *Opin. Colloid Interface Sci.* **2009**, *14*, 340–348.
- 386 (3) Paramonov, S. E.; Jun, H.-W.; Hartgerink, J. D. Self-Assembly of Peptide–Amphiphile
387 Nanofibers: The Roles of Hydrogen Bonding and Amphiphilic Packing. *J. Am. Chem. Soc.*
388 **2006**, *128*, 7291–7298.
- 389 (4) Vauthey, S.; Santoso, S.; Gong, H.; Watson, N.; Zhang, S. Molecular Self-Assembly of
390 Surfactant-like Peptides to Form Nanotubes and Nanovesicles. *Proc. Natl. Acad. Sci. U. S. A.*
391 **2002**, *99*, 5355–5360.
- 392 (5) Pashuck, E. T.; Cui, H.; Stupp, S. I. Tuning Supramolecular Rigidity of Peptide Fibers
393 through Molecular Structure. *J. Am. Chem. Soc.* **2010**, *132*, 6041–6046.
- 394 (6) Hamley, I. W. PEG-Peptide Conjugates. *Biomacromolecules* **2014**, *15*, 1543–1559.
- 395 (7) Castelletto, V.; Hamley, I. W. Self Assembly of a Model Amphiphilic Phenylalanine
396 Peptide/Polyethylene Glycol Block Copolymer in Aqueous Solution. *Biophys. Chem.* **2009**,
397 *141*, 169–174.
- 398 (8) Tzokova, N.; Fernyhough, C. M.; Topham, P. D.; Sandon, N.; Adams, D. J.; Butler, M. F.;
399 Armes, S. P.; Ryan, A. J. Soft Hydrogels from Nanotubes of Poly(Ethylene
400 Oxide)?Tetraphenylalanine Conjugates Prepared by Click Chemistry. *Langmuir* **2009**, *25*,
401 2479–2485.
- 402 (9) Tzokova, N.; Fernyhough, C. M.; Butler, M. F.; Armes, S. P.; Ryan, A. J.; Topham, P. D.;
403 Adams, D. J. The Effect of PEO Length on the Self-Assembly of Poly(Ethylene
404 Oxide)?Tetrapeptide Conjugates Prepared by “Click” Chemistry. *Langmuir* **2009**, *25*,
405 11082–11089.
- 406 (10) Diaferia, C.; Mercurio, F. A.; Giannini, C.; Sibillano, T.; Morelli, G.; Leone, M.; Accardo, A.
407 Self-Assembly of PEGylated Tetra-Phenylalanine Derivatives: Structural Insights from

- 408 Solution and Solid State Studies. *Sci. Rep.* **2016**, *6*, 26638.
- 409 (11) Dong, H.; Dube, N.; Shu, J. Y.; Seo, J. W.; Mahakian, L. M.; Ferrara, K. W.; Xu, T. Long-
410 Circulating 15 Nm Micelles Based on Amphiphilic 3-Helix Peptide–PEG Conjugates. *ACS*
411 *Nano* **2012**, *6*, 5320–5329.
- 412 (12) Hollamby, M. J. Practical Applications of Small-Angle Neutron Scattering. *Phys. Chem.*
413 *Chem. Phys.* **2013**, *15*, 10566.
- 414 (13) Heenan, R. K.; Penfold, J.; King, S. M. SANS at Pulsed Neutron Sources: Present and Future
415 Prospects. *J. Appl. Cryst* **1997**, *30*, 1140–1147.
- 416 (14) Arnold, O.; Bilheux, J. C.; Borreguero, J. M.; Buts, A.; Campbell, S. I.; Chapon, L.; Doucet,
417 M.; Draper, N.; Ferraz Leal, R.; Gigg, M. A.; *et al.* Mantid—Data Analysis and Visualization
418 Package for Neutron Scattering and μ SR Experiments. *Nucl. Instruments Methods Phys.*
419 *Res. Sect. A Accel. Spectrometers, Detect. Assoc. Equip.* **2014**, *764*, 156–166.
- 420 (15) Blondelle, S. E.; Behrouz Forood; Richard A. Houghten, A.; Pérez-Payá, E. Polyalanine-
421 Based Peptides as Models for Self-Associated β -Pleated-Sheet Complexes. **1997**, *36*, 8393–
422 8400.
- 423 (16) Cheng, P.-N.; Pham, J. D.; Nowick, J. S. The Supramolecular Chemistry of β -Sheets. *J. Am.*
424 *Chem. Soc.* **2013**, *135*, 5477.
- 425 (17) Naito, A.; Okushita, K.; Nishimura, K.; Boutis, G. S.; Aoki, A.; Asakura, T. Quantitative
426 Analysis of Solid-State Homonuclear Correlation Spectra of Antiparallel β -Sheet Alanine
427 Tetramers. *J. Phys. Chem. B* **2018**.
- 428 (18) Dong, H.; Dube, N.; Shu, J. Y.; Seo, J. W.; Mahakian, L. M.; Ferrara, K. W.; Xu, T. Long-
429 Circulating 15 Nm Micelles Based on Amphiphilic 3-Helix Peptide–PEG Conjugates. *ACS*
430 *Nano* **2012**, *6*, 5320–5329.
- 431 (19) Diaferia, C.; Mercurio, F. A.; Giannini, C.; Sibillano, T.; Morelli, G.; Leone, M.; Accardo, A.
432 Self-Assembly of PEGylated Tetra-Phenylalanine Derivatives: Structural Insights from
433 Solution and Solid State Studies. *Sci. Rep.* **2016**, *6*, 26638.
- 434 (20) Qiu, F.; Chen, Y.; Tang, C.; Zhang, J.; Gong, M.; Su, B. Self-Assembling Surfactant-like
435 Peptide A6K as Potential Delivery System for Hydrophobic Drugs. *Int. J. Nanomedicine*
436 **2015**, *10*, 847.
- 437 (21) Adams, D. J.; Holtzmann, K.; Schneider, C.; Butler, M. F. Self-Assembly of Surfactant-like
438 Peptides. *Langmuir* **2007**, *23*, 12729–12736.
- 439 (22) Song, Z.; Chen, X.; You, X.; Huang, K.; Dhinakar, A.; Gu, Z.; Wu, J. Self-Assembly of
440 Peptide Amphiphiles for Drug Delivery: The Role of Peptide Primary and Secondary
441 Structures. *Biomater. Sci.* **2017**, *5*, 2369–2380.
- 442 (23) Capes, J. S.; Kiley, P. J.; Windle, A. H. Investigating the Effect of PH on the Aggregation of
443 Two Surfactant-Like Octapeptides. *Langmuir* **2010**, *26*, 5637–5644.
- 444 (24) Novelli, F.; De Santis, S.; Diociaiuti, M.; Giordano, C.; Morosetti, S.; Punzi, P.; Sciubba, F.;
445 Viali, V.; Masci, G.; Scipioni, A. Curcumin Loaded Nanocarriers Obtained by Self-
446 Assembly of a Linear d,l-Octapeptide-Poly(Ethylene Glycol) Conjugate. *Eur. Polym. J.*
447 **2018**, *98*, 28–38.
- 448 (25) Castelletto, V.; Gouveia, R. J.; Connon, C. J.; Hamley, I. W.; Seitsonen, J.; Ruokolainen, J.;
449 Longo, E.; Siligardi, G. Influence of Elastase on Alanine-Rich Peptide Hydrogels. *Biomater.*
450 *Sci.* **2014**, *2*, 867–874.

- 451 (26) Lawrence, P. B.; Price, J. L. How PEGylation Influences Protein Conformational Stability.
452 *Curr. Opin. Chem. Biol.* **2016**, *34*, 88–94.
- 453 (27) Castelletto, V.; Newby, G. E.; Hermida Merino, D.; Hamley, I. W.; Liu, D.; Noirez, L. Self-
454 Assembly of an Amyloid Peptide Fragment–PEG Conjugate: Lyotropic Phase Formation and
455 Influence of PEG Crystallization. *Polym. Chem.* **2010**, *1*, 453.
- 456 (28) Yang, S. J.; Zhang, S. Self-Assembling Behavior of Designer Lipid-like Peptides. *Supramol.*
457 *Chem.* **2006**, *18*, 389–396.
- 458 (29) Nagai, A.; Nagai, Y.; Qu, H.; Zhang, S. Dynamic Behaviors of Lipid-like Self-Assembling
459 Peptide A6D and A6K Nanotubes. *J. Nanosci. Nanotechnol.* **2007**, *7*, 2246–2252.
- 460 (30) Wang, J.; Han, S.; Meng, G.; Xu, H.; Xia, D.; Zhao, X.; Schweins, R.; Lu, J. R. Dynamic
461 Self-Assembly of Surfactant-like Peptides A6K and A9K. *Soft Matter* **2009**, *5*, 3870.
- 462 (31) Lee, E. S.; Shin, H. J.; Na, K.; Bae, Y. H. Poly(l-Histidine)–PEG Block Copolymer Micelles
463 and PH-Induced Destabilization. *J. Control. Release* **2003**, *90*, 363–374.
- 464 (32) Valéry, C.; Paternostre, M.; Robert, B.; Gulik-Krzywicki, T.; Narayanan, T.; Dedieu, J.-C.;
465 Keller, G.; Torres, M.-L.; Cherif-Cheikh, R.; Calvo, P.; *et al.* Biomimetic Organization:
466 Octapeptide Self-Assembly into Nanotubes of Viral Capsid-like Dimension. *Proc. Natl.*
467 *Acad. Sci. U. S. A.* **2003**, *100*, 10258–10262.
- 468 (33) Mandal, D.; Nasrolahi Shirazi, A.; Parang, K. Self-Assembly of Peptides to Nanostructures.
469 *Org. Biomol. Chem.* **2014**, *12*, 3544–3561.
- 470 (34) Qiu, F.; Chen, Y.; Tang, C.; Zhao, X. Amphiphilic Peptides as Novel Nanomaterials: Design,
471 Self-Assembly and Application. *Int. J. Nanomedicine* **2018**, *13*, 5003–5022.

472

473